actuators

MDPI

Article

Hybrid Solenoids Based on Magnetic Shape Memory Alloys

Manuel Mauch, Marco Hutter and Bernd Gundelsweiler *

Institute of Design and Production in Precision Engineering (IKFF), Faculty 7—Engineering Design, Production Engineering and Automotive Engineering, University of Stuttgart, Pfaffenwaldring 9, 70569 Stuttgart, Germany; manuel.mauch@ikff.uni-stuttgart.de (M.M.); marco.hutter@ikff.uni-stuttgart.de (M.H.)
* Correspondence: bernd.gundelsweiler@ikff.uni-stuttgart.de

Abstract: The mobility of today and tomorrow is characterized by technological change and new challenges in drive concepts such as electric or hydrogen vehicles. Abolishing conventional combustion engines creates even more need for switching or valve technology in mobility systems. For switching and controlling purposes, solenoids are used in large numbers and in a wide variety of applications, thus making a significant contribution to the overall success of the energy transition, and not only in the automotive sector. Despite their long existence, continued research is being carried out on solenoids involving new materials and actuator concepts. Great interest is focused on providing an adjustable force–displacement characteristic while simultaneously reducing the noise during switching. At IKFF, research is being conducted on hybrid electromagnets in the border area of switching and holding solenoids. This paper aims to present the major advantages of this hybrid drive concept based on an electromagnetic FEA simulation study of two drive concepts and specially developed and characterized prototypes with magnetic shape memory (MSM) alloys. The concepts differ in the spatial orientation of the MSM sticks to generate an active stroke of the plunger, which contributes to a beneficial force–displacement characteristic and lower power consumption while minimizing switching noise.

Keywords: precision engineering; hybrid actuator; switching-holding solenoid; magnetic shape memory alloy

Citation: Mauch, M.; Hutter, M.; Gundelsweiler, B. Hybrid Solenoids Based on Magnetic Shape Memory Alloys. *Actuators* **2023**, *12*, 328. https://doi.org/10.3390/act12080328

Academic Editors: Todor Stoilov Todorov, Rosen Mitrev and Wei Min Huang

Received: 12 July 2023
Revised: 11 August 2023
Accepted: 13 August 2023
Published: 15 August 2023

1. Introduction

1.1. Motivation

A solenoid is an electromechanical device that converts electrical energy into linear or rotational motion. The functionally relevant elements of solenoids are the iron circuit for flux guiding, the coil for generating the magnetic field due to an applied current, and the air gap in which the energy conversion takes place. Solenoids are used in a wide range of applications, including valves, locks, and actuators. Two fundamentally different designs of solenoids are the switching and the holding solenoid. A switching solenoid, shown in Figure 1 on the left, is designed to operate as an on–off switch, meaning it is either fully open or fully closed. These can be used, for example, in relay technology. The stroke of the plunger is usually in the range of a few millimeters with a force sufficient to start the plunger's movement in the rear-end position. On the other hand, a holding solenoid is designed to hold a position or maintain a force, rather than switching on and off. The basic design is shown in Figure 1 on the right. Here, the generated stroke is just a fraction of what switching solenoids are capable of. A common challenge for a holding solenoid is the low force at maximum air gap and the difficulty overcoming the counter force of the spring. However, the generated force of a holding solenoid at closed stage is higher than the force of a switching solenoid, which is beneficial for holding tasks. If a user has multiple applications simultaneously which require a large attraction force combined with a relatively large air gap, hybrid electromagnets such as those developed at IKFF can be utilized as the actuators [1–4].

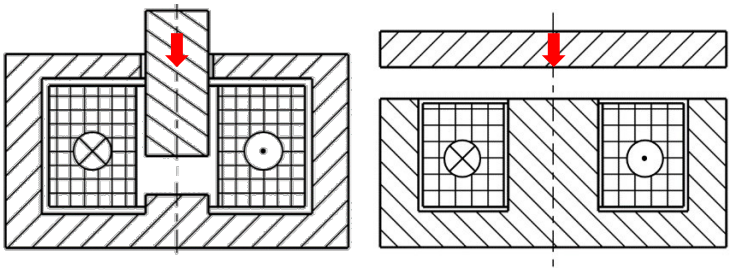

Figure 1. Differentiation of holding and switching solenoids [1]. The red arrow indicates the force due to reluctance action and thus the direction of movement of the core (**left**) or armature (**right**).

The aim of these actuators is to obtain a larger force with a larger air gap. Of course, because of energy conservation, it is not possible to increase the overall mechanical work done by the solenoid. Therefore, the following equation applies for modified characteristic curves.

$$W_{mech} = \int_{\delta_{min}}^{\delta_{max}} F_m(\delta)\, d\delta, \tag{1}$$

Due to the individual design of the magnetic circuit with corresponding air gap lengths and cross-sectional areas of ferromagnetic components of the solenoid, switching solenoids and holding solenoids differ in the force–air gap characteristic, which is shown in Figure 2. In case of a switching solenoid, the force–air gap characteristic can be actively changed by influencing the characteristic curve through cone control, see Figure 3 For holding solenoids, on the other hand, the relation

$$F \sim \frac{1}{\delta^2} \tag{2}$$

is predominant, which explains the exponential increase in force of a holding solenoid system with decreasing air gap.

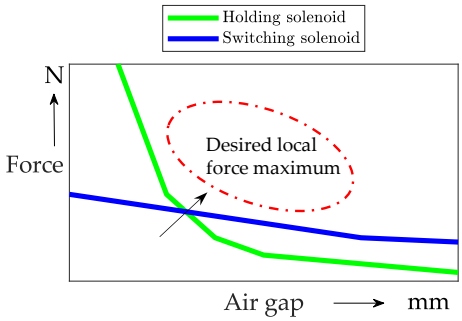

Figure 2. Region of desired local force maximum in relation to characteristic curves of holding and switching solenoids.

However, if the force–air gap characteristic with its maximum is shifted into the preferred range, shown in Figure 2, it is possible to attract an armature plate at a larger air gap, thus avoiding a major disadvantage of holding solenoids in general.

The solenoids presented in this paper use NiMnGa-based MSM alloys in the form of sticks. These active elements show a large deformation of around 6% perpendicular to an external magnetic field, due to reorientation of the martensitic lattice [5]. As the energy density of MSM alloys is high, they can additionally exhibit stress up to 2.0 N/mm^2 at full elongation [6], rendering them well suited for use in miniaturized systems. The elongation has been investigated for a number of actuation and positioning applications [7,8] and is used here to create an active stroke of the plunger towards the armature. The focus lies in the design of the spatial orientation of the MSM sticks and whether a horizontal or vertical alignment of the sticks is to be preferred for a beneficial force–displacement characteristic.

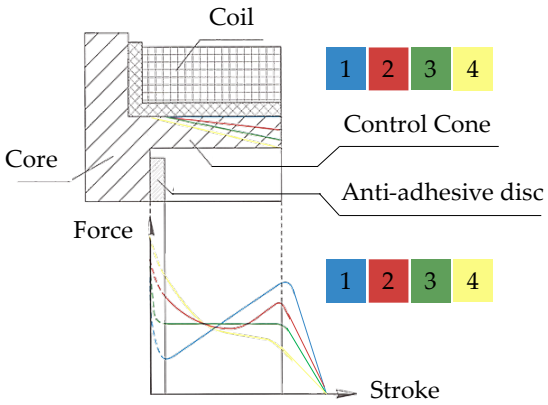

Figure 3. Adjustment of the qualitative characteristic curve of a switching solenoid using a control cone ([9] modified by M. Mauch; cropped, translated details and enlarged legend).

1.2. Content Overview

For better clarity and presentation of the results of this paper, a short outline of the contents is given here.

After a concise introduction and discussion of the motivation in Section 1, Section 2 provides a brief explanation of the influence on the characteristic curves of solenoids. These can have mechanical as well as control–technical contents. Additionally, part of that chapter is a fundamental contribution to the subject of magnetic shape memory alloys. The Matlab/Simulink model presented in Section 3 for describing the actuator principle forms the basis for deriving hypotheses for the actuator development process. Furthermore, the sequence in the switching process of an actuator with an active core is presented. One of the main focuses of the paper is found in Section 4, where a detailed simulation study of two setups is covered. The two setups are presented, and an overview of the varied parameters is given. Then, the results of the simulation study, including derivation of force and flux density distribution, are presented. The flux density distribution in the MSM sticks is then shown in Section 5, in which the developed prototypes are presented as another main emphasis of this paper. The prototypes were each developed from a conceptual phase in which translational motion transformation for one setup and magnetic circuit optimization for the other were part of the investigation. Section 6 first presents the two measurement setups used for characterization of the two setups and then discusses the measurement results for force–displacement (static testing) and current–displacement (dynamic testing). Section 7 concludes this paper, summarizing and discussing the results and providing an outlook for further research.

2. State of the Art

2.1. Methods for Influencing the Characteristic Force–Displacement Characteristics of a Solenoid

The behavior of the magnetic force–displacement characteristics can be influenced within limits by appropriate design of the magnetic circuit, as can be seen in Figure 3.

The magnetic force–displacement characteristic depends primarily on the design of the air gap and the ferromagnetic parts of the magnetic circuit (armature/plunger and its counterpart) surrounding the air gap. All operations that lead to a selective change in the magnetic force–displacement characteristic by modifying the geometry of the air gap, armature and armature counterpart are referred to as geometric characteristic influencing or cone control, shown in Figure 2. This technology works through the target-orientated magnetic saturation of explicit parts of the solenoid.

Geometric characteristic influencing makes it possible to adapt the force–displacement characteristic to the specific application to meet the technological requirements of the use case. Compared to solenoids without geometric characteristic influencing, solenoids that adapt modifications of the magnetic circuit allow much better utilization of the available mechanical work, especially for large strokes. Therefore, it is very common in switching

solenoids, which have a significant stroke of the plunger, and it is not used for holding solenoids, which usually only perform a stroke on a much smaller scale. In addition to an improvement in static behavior, as the mentioned force–displacement characteristic, changes in dynamic behavior are also made possible through characteristic curve influence. These changes in dynamic behavior involve a change in the mechanical motion behavior as a result of a changed magnetic force–displacement characteristic. Dynamic changes can be seen by observing switching currents or required switching time [10].

The dynamic behavior of a DC solenoid can furthermore be modified by adapting the solenoid's drive system to the load case. For example, this can be made possible by increasing the activation power by rapid-excitation or overexcitation circuits. The overexcitation has an influence on the dimensioning of the coil [10].

2.2. Basics of MSM Alloys

MSM materials are a group of materials that exhibit deformation under influence of a magnetic field. The deformation is caused by magnetically induced reorientation (MIR) in the martensitic lattice structure of these alloys. The unit cell of typically employed alloys has a tetragonal shape, with the axes not only of different lengths but also different permeabilities. Therefore, an external magnetic field can cause unit cells to switch from one twin variant to the other, by aligning the short or magnetically easy axis with the magnetic field vector. Subsequently, the long axis is oriented perpendicular to the external field, yielding an elongation suitable for use in an actuator in this direction [11].

To exploit these mechanics in actuators, MSM alloys are typically of cuboid shape, made from single crystal. These MSM sticks maximize the transfer of magnetically induced strain (MFIS) into stroke along their long axis. The other dimensions are kept small to reduce volume and magnetic resistance, as permeability of the alloy ranges from 2 . . . 50 [6], depending on the crystal axis, and is therefore considerably smaller than typical flux guidance materials.

Most commonly, NiMnGa alloys with a maximum strain of 6% for stresses up to 2.0 N/mm^2 and a blocking stress of around 3.5 N/mm^2 are investigated [6]. In combination with their high energy density, these alloys offer potential for application in compact actuators. To achieve desired elongations, magnetic excitation needs to be sufficient. Figure 4 shows the field strain characteristic in relation to mechanical load, as given by the manufacturer. The material's ability to reach full or near-full elongation at loads up to 2.0 N/mm^2 for flux densities of 0.6 . . . 1.0 T within the alloy can be seen.

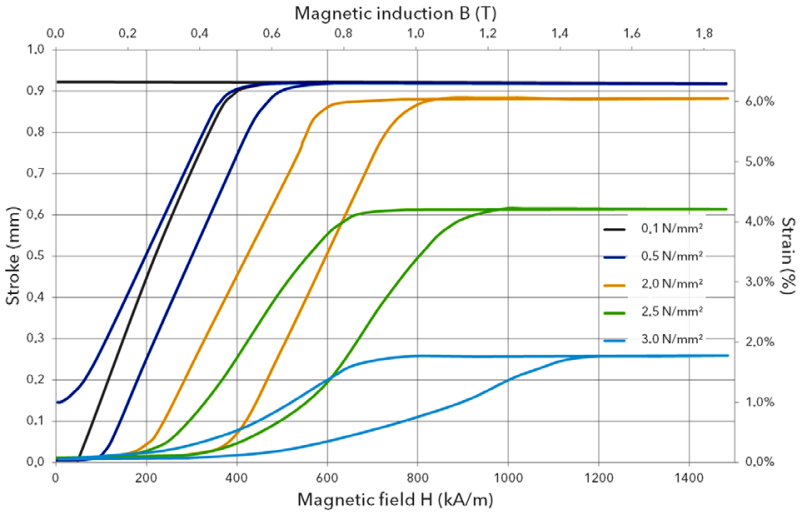

Figure 4. MSM elongation scheme and stroke–excitement characteristic ([6] modified by M. Mauch; translated details).

The hysteresis in the graph is caused by the twinning stress, a resistance of the lattice structure to any shape change, and is typically in the order of 0.5 N/mm^2. This needs to be overcome by either magnetic excitement or mechanical load to achieve deformation, enabling the use of MSM for dampers and in multi-stable systems [12,13].

Due to the mechanics of the microstructure reorientation, compression by magnetic field requires the excitation field to rotate by 90°. Implementation of this solution puts greater demands on the design of the magnetic circuit, with the possible need to include additional excitation coils, but it is in some cases also pursued [14]. The mode of operation most commonly employed in MSM-based actuator design is elongation by magnetic excitation and compression by an external mechanical load provided by a spring or gravitational force [15]. This configuration can be used to create a push actuation from the MSM elongation, which has most widely been transferred to fluidic applications, such as valves [16,17], but has potential for other areas like automation engineering as well [18]. Additionally, MSM-based systems employing other operational principles have been explored. Among these are the combination of two MSM sticks for an antagonistic push–push actuator [19], localized deformation of the MSM stick as a microfluidic pump [20] and combination of permanent magnetic and electromagnetic excitation with a magnetic counterforce [21].

3. Modelling of the Actuator Concept and Derivation of Performance Expectations

To create a hypothesis about the behavior and the expected characteristic curves of hybrid switching–holding actuators with an active core before the large-scale magnetic FEA simulation and prototype development, a simplified general structure of such an actuator was modelled in Matlab/Simulink (Matlab/Simulink version 2022a).

3.1. Matlab/Simulink Model of the Actuator Concept

In the model, how exactly the extension of the core takes place was neglected, and no consideration was given to volume consistency of the core. In the built prototypes, this elongation was finally enabled via elongation of the implemented MSM stick in the presence of a magnetic excitation. Based on the proven network method for magnetic circuits, and a derived equivalent circuit with electrical, magnetic and mechanical subsystem and associated differential equation system, the model is shown Figure 5a.

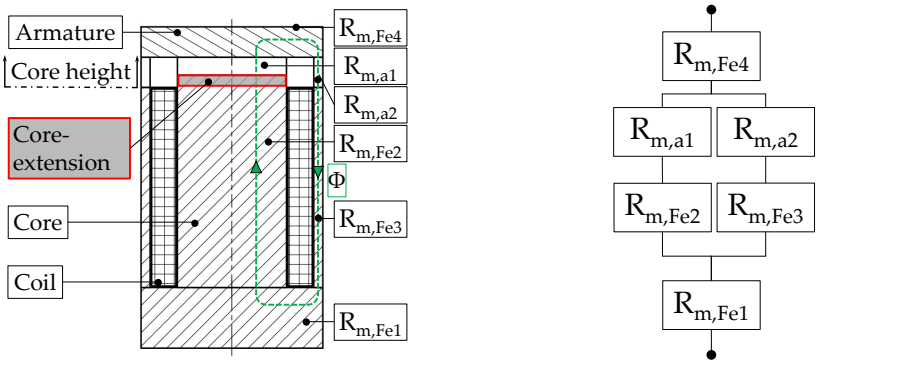

(**a**) Modelling of the solenoid (**b**) Network of the magnetic circuit

Figure 5. Modelling of a simplified solenoid with elongated inner core and corresponding magnetic circuit. The labels indicate a correlating magnetic resistance R_m for ferromagnetic parts, e.g., $R_{m,Fe4}$, or for the air gap, e.g., $R_{m,a1}$. According to their length, cross-sectional area and material, these magnetic resistances can be determined approximately [10].

The model describes a conventional, rotationally symmetric solenoid, considering simplifications, whose inner core is designed to be variably adjustable regarding its height. The network of the magnetic circuit can be seen in Figure 5b. Based on this network of equivalent magnetic resistors, a total magnetic resistance was calculated, which is the basis for obtaining the total magnetic flux. Material data for the flux-guiding parts was also implemented to examine magnetic saturation effects. The magnetic flux further

provides Maxwell's tensile force, which is passed to the mechanical subsystem, in which a spring is located, and suspension and damping are taken into account. The spring and suspension/damping inhibits the movement of the armature at all times. Finally, the movement of the plunger was reconstructed and evaluated from this system. In the model, it is assumed that the core in the rotationally symmetric solenoid is extended beyond the solenoid's core height (see Figure 5a). This was done starting with a reference setup with an extension of 0 mm up to an active core extension of 1 mm in 0.2 mm steps. The modeling up to an active stroke of 1 mm was because this corresponds to the direct active elongation of the MSM stick used in the actual prototypes developed in Section 5, which equals 5–6% of the initial length of 20 mm. Any transmission of the extension movement in the structure with the horizontally orientated MSM stick was not investigated at this point, and therefore no extension of the core height in the modelled solenoid exceeded 1 mm here.

3.2. Performance Expectations of the Solenoid

Thus, with an active stroke of the core, it can be assumed that the rise of the force–displacement characteristic shifts toward a larger air gap due to the actively shortened air gap (see Figure 6a). Furthermore, it is apparent that the current–displacement characteristic also shows a beneficial influence of the enabled core extension, as can be seen in Figure 6b. The switching current required for an explicit air gap decreases with the amount of core extension.

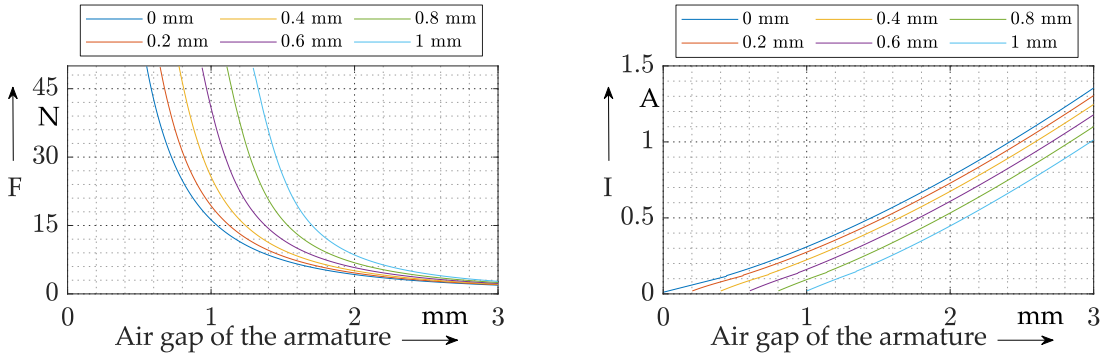

(**a**) Force–displacement correlation (**b**) Current–displacement correlation

Figure 6. Expected force–displacement and current–displacement characteristics according to modelling. The different curves illustrate correlating core extensions, irrelevant to the physical principle responsible for the core's extension. Research in which the extension of the core was realized via the design of the solenoid as a reluctance actuator without the use of MSM sticks has shown similar behavior of the characteristic curves [4]. In the presented study, this extension of the core is realized using MSM sticks.

3.3. Presentation of the Basic Switching Principle

The basic principle of both actuators shown in this article is illustrated in Figure 7. The design shown in this sequence does not contain any MSM sticks since the basic switching operation of a switching/holding solenoid with active core is independent from the actual physical principle driving its extension. In [4], the movement of the core is enabled due to reluctance force, for example. In this paper, however, MSM elements were at the center of investigations and were used to drive the plunger in its front-end position. It was further investigated whether a horizontal and/or vertical orientation of the MSM element is advantageous. Therefore, only the basic principle of the active core with its extension is emphasized in Figure 7, without already specifying a favorable orientation in the shown principle of a switching operation.

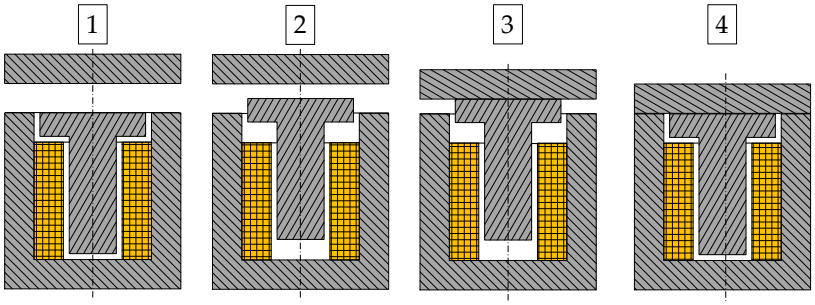

Figure 7. Principle of the basic switching operation of a switching/holding solenoid.

At the beginning, all components are in initial position and the coil is energized (step 1, initial stage). Subsequently, a magnetic field builds up which causes the MSM stick (not shown in Figure 7) to elongate, resulting in a vertical movement of the plunger towards the armature (step 2, activated stage). In the actual prototypes, this stroke was limited by the elongation of the MSM sticks (1 mm for vertical and 1.7 mm for horizontal alignment of the MSM stick due to defined transmission).

The actively shortened air gap to the armature and the resulting smaller magnetic resistance of the alignment causes the armature to move toward the solenoid's body (step 3) due to Maxwell's tensile force. Depending on how big the actual air gap is and what active stroke the plunger can perform, these initially independent movements can also happen simultaneously to some extent, which positively affects switching times. When reaching the solenoid's body, the armature is dampened due to the compression of the MSM stick, which happens to have a beneficial influence on the switching noise. The switching process is then terminated as soon as the armature reaches its end position (step 4, closed stage), and the plunger is deferred to the initial position. The spring for resetting the armature is not shown in the illustration. Yet, after resetting, another switching process can be executed. Since this principle always requires full elongation of the MSM sticks, no dedicated control scheme is necessary. The entire actuator can be supplied with a simple voltage step, providing the field for MSM stick actuation and armature attraction.

4. Simulation Study with Two Different Actuator Variants

To establish a more detailed understanding of the properties of actuators based on the principle described above, after modelling the system in Matlab/Simulink, an FEA-based magnetostatic simulation study is conducted.

4.1. Materials and Methods

To reduce system complexity, 2D simulations conducted in this chapter were executed using an FEA tool (ANYSY Electronic Desktop 2022R1 (MAXWELL 3D-design for magnetostatic solver)). At the core of each setup was a single MSM stick made of Magnetoshape [8] with a length of 20 mm and a cross section of 3×5 mm^2. Results were generated for a magnetostatic approach and evaluated numerically using Matlab/Simulink version 2022a. Dynamic components of actuator behavior were not explored with the magnetostatic approach, as the simulation software did not allow for independent movement of two components, which would have been necessary here. Dynamic behavior was, however, characterized experimentally, as discussed in Section 5.1.

4.2. Introduction of the Two Actuator Setups

Using MSM sticks to enable a specific plunger movement, a distinction can be made between a vertically or a horizontally aligned MSM stick resulting in two different variants regarding the common orientation of the coil.

This study aimed to find ranges of key properties and beneficial use cases for both variants, and eventually to find two suitable designs for each concept while deriving

first prototypes. The 2D FEA simulation models for both variants with an MSM stick in black and yellow at their center are shown in Figure 8.

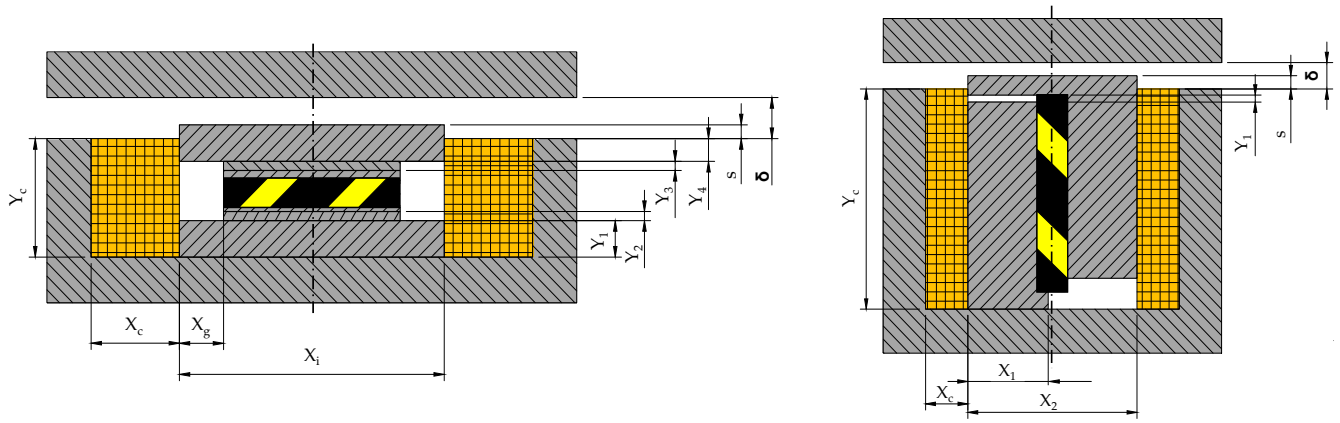

(**a**) Horizontal setup (**b**) Vertical setup

Figure 8. Simulation setups with varied design parameters. The parameters describing the dimensions of the actuator in the horizontal x-plane are clarified by an x, the dimensions in the vertical rotation plane are characterized by a y. For comparability reasons, the coil is parameterized with a subscript c in both vertical and horizontal design, whereas design parameters vary in their denotation due to their differences in design. Furthermore, the parameter s represents the stroke of the plunger and δ represents the air gap. All parameters with their considered ranges are included in Tables 1–3.

The MSM sticks' depth of 5 mm was used to define the theoretical depth for both actuator variants in the 2D FEA simulation since this was the minimal possible dimension for each design. Exterior to the stick, the magnetic circuit was designed to create and guide the magnetic flux considering the correct orientation of the generated magnetic field (vertical magnetic field orientation for horizontally aligned sticks and horizontal magnetic field orientation for vertically aligned sticks) to enable the sticks' elongation according to Section 2.2.

Table 1. Parameter variations (mm) in the dimensions of the flux guidance.

	X_g	X_i	Y_4	Y_3	Y_2	Y_1	X_2	X_1	Y_1
Vertical	-	-	-	-	-	-	10 . . . 20	0 . . . 8.5	0 . . . 2
Horizontal	3 . . . 9	26 . . . 38	2 . . . 10	1 . . . 5	1 . . . 5	2 . . . 10	-	-	-

Table 2. Parameter variations (mm) of the geometric dimensions of the coil.

	Y_c	X_c
Vertical	25 . . . 35	5 . . . 15
Horizontal	9 . . . 33	10 . . . 16

Table 3. Parameter variations (mm) for the upper and lower end positions of the armature.

	d	s
Vertical	0 . . . 1.5	0 . . . 1
Horizontal	0 . . . 1.5	0 . . . 1

4.3. Parameter Variations

The simulations were intended as parametric studies to give a broader understanding of the actuators' behavior depending on their design. The simulation models and the geometric parameters are displayed in Figure 8. The parameter variations can be divided into different groups:

1. Variations in the dimensions of the flux guidance were intended to find suitable magnetic excitation within the MSM stick while avoiding undesired flux paths and saturation effects. The dimensions of the armature and the solenoid's body were not varied for either variant but were fixed at a value of 4 mm to rule out magnetic saturation within the limits of the specific electrical excitation.
2. Geometric dimensions of the coil and the current density applied were varied to find both the necessary excitation for a sufficient magnetic flux in the MSM stick and the relation of force created to applied excitation.
3. Upper and lower end positions of the armature and plunger movements were combined to create initial, activated and closed states of the switching operation of the actuator. For the concept with a horizontally aligned MSM stick, transmission was not enabled, and the stroke of the plunger was identical to the vertical variant.

In the initial stage (step 1 in Figure 7), the air gap of the armature is at its maximum at 4 mm and the plunger is not extended, as the MSM stick has not yet elongated. In the activated stage, the plunger has extended due to the elongation of the MSM stick, but the armature still remains in rear-end position (step 2 in Figure 7). The contact stage, step 3 in Figure 7, was not looked at in detail regarding strong transient effects at this specific point in the switching process. For further detail, a transient magnetic FEA simulation might help in describing the system. However, the touching of the two parts is nevertheless going to be difficult to grasp. The different directions the elements are moving as they move towards each other causes problems in FEA simulations. In the closed stage (step 4 in Figure 7), armature and plunger are in their respective front- or rear-end position with the MSM stick compressed. During steps 1–3, the increase in force on the armature caused by the plunger's movement can be determined; according to the first modelling results, this is expected to be a core characteristic of this type of actuator. At closed state, the maximum force can be evaluated and used as a metric to determine force density of the design in general.

As the simulation presented here was intended to give an abstract overview of the potential characteristics of the actuator principle, several more simplifications were made. The deformation of the MSM sticks was not modelled, but the magnetization characteristic of the material's axes was adjusted to represent the correct configuration regarding the elongated or compressed state the MSM stick was in. Additionally, the movement of the plunger was implemented by simply increasing the height of the ferromagnetic core by 1 mm (depicted as parameter Y in Figure 8), corresponding to a strain of 5% of the initial length of the MSM stick. Any details of a specific mechanism of the plunger's movement were omitted at this point. However, as the horizontal configuration needed a mechanism for redirecting stick motion for transmission, bilateral spacing was provided on either side of the MSM stick.

The ranges of parameter variation were chosen arbitrarily, but with the aim of maintaining comparability between the horizontal and vertical setups. This was true for both the overall actuator volume and the magnetic excitation given by the coil's cross section and current density, which were both used for evaluation of the simulation results. They were considered in combinations with the force on the armature and the magnetic flux going parallel to the short side of the MSM sticks.

4.4. Evaluation of the Flux Density in the MSM Sticks

As sufficient flux density within the MSM stick is essential for the intended actuator function, it was an aim to find the effectiveness at which the variants were creating the required magnetic field. These results are displayed in Figure 9 as the flux density within the MSM stick over the magnetic excitation in Amperewindings (AW) on the top and actuator volume on the bottom for both the horizontal (a) and vertical (b) setups.

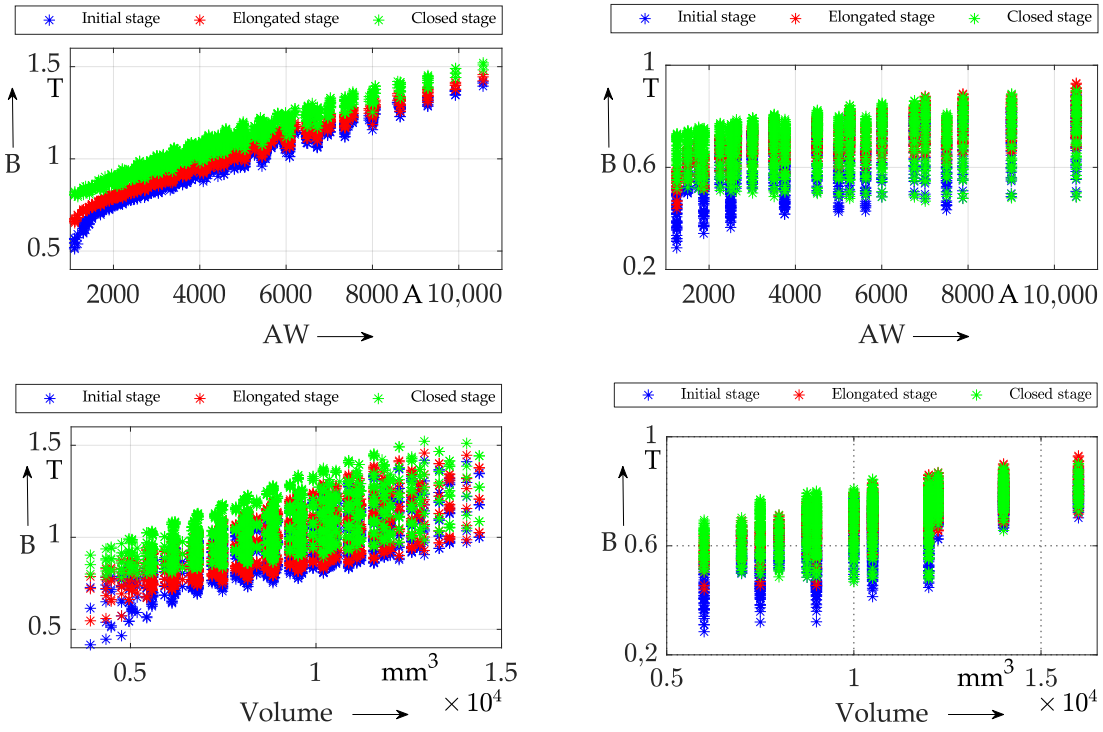

(**a**) Horizontal setup (**b**) Vertical setup

Figure 9. Simulation results: correlation flux density (B) and excitation (AW), and correlation flux density (B) and actuator volume (mm^3), for both horizontal (**a**) and vertical (**b**) setups.

As can be seen from the graphs, there were clear differences between the setups. Looking at the flux density (B) over excitation (AW), the results for the vertical setup showed lower overall flux densities at similar magnetic excitation, as well as a wider spread of results. This indicated that design of the flux guidance was more important for this setup, as is to be expected due to the necessary redirection of flux within the core. As for the behavior of the horizontal setup, the overall higher flux densities fell in two mostly linear sections, divided by a bend. Flux density at this bend corresponded with the saturation of the MSM easy axis.

Despite the saturation in many of the evaluated variants, flux densities were significantly higher for the horizontal setup at comparable actuator volume. This was further indication of the simpler setup of the magnetic circuit for the horizontal setup and suggested more potential for miniaturization.

What all the plots above show is the influence of the stage in the switching operation of both actuators on the flux density. Later stages of the operation showed a generally higher flux density, which is to be expected from the air gaps closing and the changes in MSM stick permeability. This was most pronounced in the depiction of flux density (B) over excitation (AW) for the horizontal setup. In contrast, the results for the vertical setup did not indicate a clear change in the maximum of flux density (B) between activated and closed stage, and even showed a greater spread of results for the closed stage. This indicated a greater impact of the reluctance of the often unsaturated MSM stick in these setups.

4.5. Evaluation of the Force on Armature

Force on the armature was the second metric for evaluation in this study. Results are displayed in Figure 10 (top) as force (F) over magnetic excitation (AW) and force (F) over actuator volume (bottom) for the horizontal (a) and vertical (b) setups.

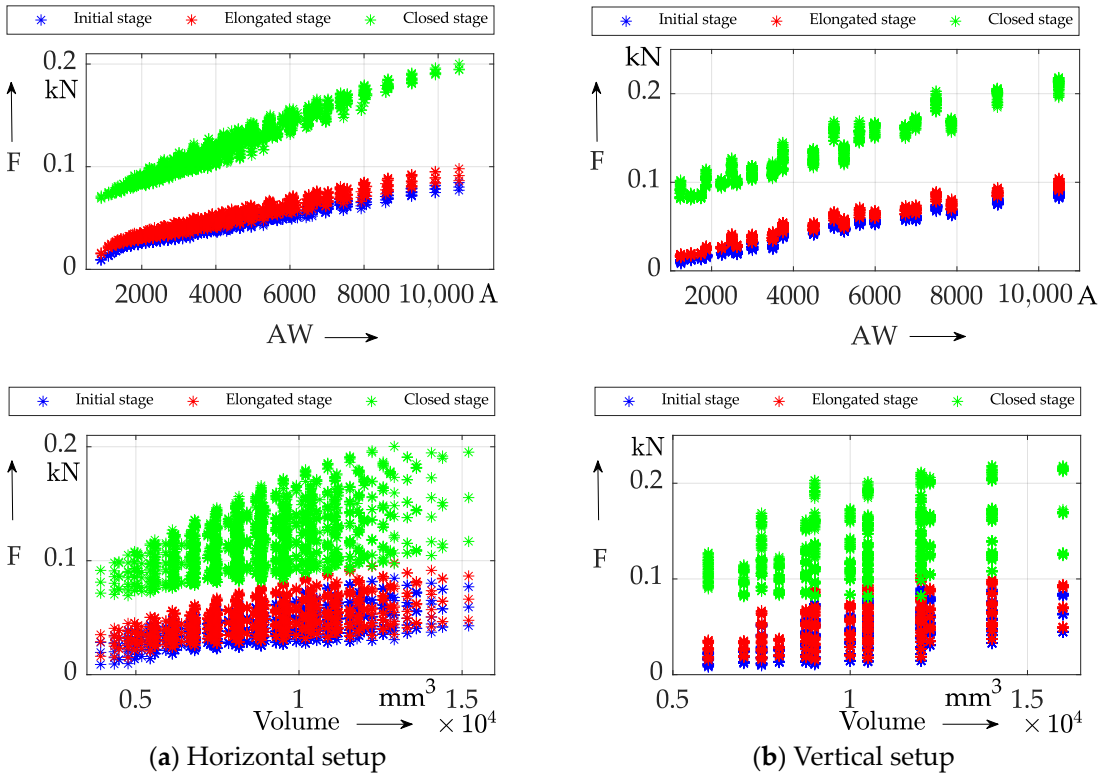

(**a**) Horizontal setup (**b**) Vertical setup

Figure 10. Simulation result: correlation force (F) and excitation (AW) and correlation force (F) and actuator volume (mm^3) for both horizontal (**a**) and vertical (**b**) setups.

Differences between the figures were less distinct than for the flux density results. For both setups, excitation was dominant for determining actuator force. However, actuator volume appeared to have a stronger influence on actuator force for the horizontal setup over the whole of the volume range. For the vertical setup, there was a visible increase until about 1800 mm^3. After that point, maximum force changed only marginally if at all, while minimum force still increased. Overall, force ranges were similar between the two setups. However, the horizontal setup showed a slowed rate of increase with excitation over around 1500 AW, similar to that found for the magnetic flux density, as is visible in Figure 9a. This was attributed to the same saturation effect in the MSM stick as mentioned above. In combination, this indicated a more efficient use of the horizontal setup for lower excitation and therefore potentially more miniaturized actuator systems.

The influence of the stage in the switching cycle was also apparent, with forces in the activated and especially the closed stages higher than in the initial stage. The difference between initial and activated stage was also a simulative proof of concept. Since there was, however, clear overlap between these two stages, the ratio in force from initial to activated stage was calculated. The maximum, minimum and average of this ratio for both setups are displayed in Table 4.

Table 4. Attainable amplification factors for the armature force as derived from the simulation.

	Horizontal	**Vertical**
Avg	1.1599	1.2409
Max	1.8084	1.8145
Min	1.0950	1.0976

As the ratio was greater than one in all cases investigated here, the plunger movement always led to an increase in force on the armature. The minimum and maximum increase

was similar between both setups; however, the average was higher for the vertical setup. This indicated a greater number of variants towards the upper limit of the force ratio range.

In conclusion, the capability of both setups to achieve the central desired function of the actuator principle was shown and the hypothesis of the Matlab/Simulink model could be confirmed. The MSM sticks can be supplied with sufficient magnetic flux for full elongation and extension of the plunger always leads to an increase in force on the armature. Additionally, expectations about the design were met, in that ensuring sufficient flux in the MSM stick is more challenging in the design of the setup with vertical sticks. With the available simulation program, it was not possible to model the force–displacement characteristic of the entire switching process, which consists of an individual movement of both the plunger and the armature. Therefore, as discussed in the following section, prototypes were developed and their force–displacement characteristics were obtained by measurement.

5. Prototypes

To verify the results from the simulation study of the previous chapter, and to acquire the respective force–air gap characteristic, two prototypes, one for each setup, were developed, as discussed in this chapter. Development of the prototypes consisted of designing the magnetic circuit as well as considerations of mechanical guidance for the moving parts of the actuators. The prototypes were subsequently built and experimentally characterized. The aim of developing both prototypes was to create proofs of concept for each setup and the necessary subsystems rather than a direct comparison with regards to common design goals.

5.1. Materials and Methods

For both prototypes, the same type and number of MSM sticks were used, as a common starting point of design. These were two sticks with dimensions of $3 \times 5 \times 20$ mm^3 made from Magnetoshape [6] with a maximum strain of 6%. The choice of two sticks was advantageous to make use of symmetry in the actuator design. In both cases, mountings based on polymer flexures were used to implement the sticks, as they secured the sticks in position, as well as guiding their elongation movement [22]. Additionally, both prototypes were developed as cylindrical actuators, as commonly seen in solenoids.

The development of the prototypes made use of CAE software (Autodesk Fusion 360 2.0.16486 x86_64) and an FEA simulation tool (ANYSY Electronic Desktop 2022R1 (MAXWELL 3D-design for magneto-static solver) in the methodology process because of their availability. These can of course be substituted by other software on the market.

5.2. CAE Prototyping for the Horizontal Setup

Design of a prototype for the setup with horizontal sticks needed to consider the redirection of MSM stick elongation in the design process in addition to the magnetic circuit and movement guidance, as mentioned above. The two sticks were set in the same plane, with their fixed and loose stops on opposite ends, respectively. Therefore, the plunger movement was initiated at two diametrically opposed points, reducing the chance of the plunger tilting and consequently reducing the requirements for guiding the movement.

Between the MSM sticks and the plunger, the redirecting of movement needs to happen. There are a multitude of possible mechanisms for this, such as wedges, flexure kinematics or hydraulics. Figure 11 gives an overview of six distinct mechanisms. Since the redirection of movement is required, it also is possible to incorporate a transmission ratio other than 1:1 without the need of additional components. This is possible for all the mechanism principles shown below.

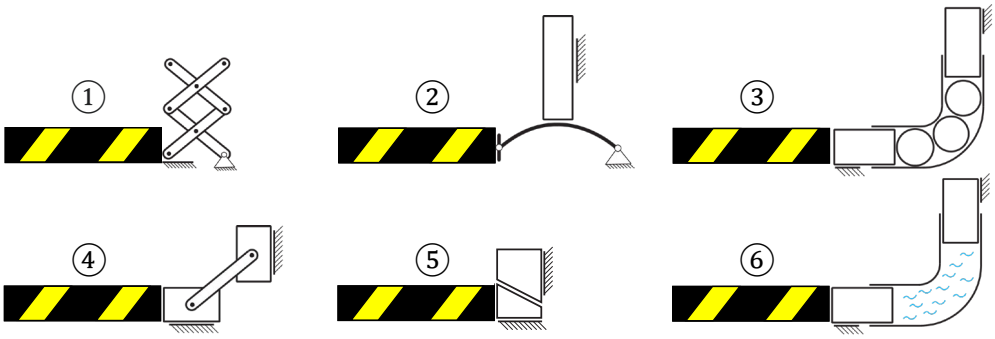

Figure 11. Translation of the MSM stick's elongation from a horizontal to a vertical movement. Lifting platform (①), Flexure (②), Bent tube with balls (③), Sliding joint (④), Inclined plane (⑤), Bent tube with fluid (⑥).

For the prototype in this work, a ball and wedge mechanism was chosen, which is shown in Figure 12.

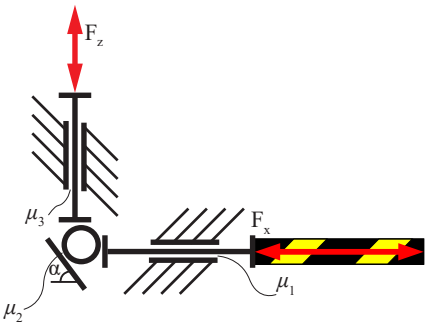

Figure 12. Transmission used in the horizontal setup.

The MSM sticks pressed against a pin in a sleeve bearing (F_x). The pins then moved a bearing ball along an inclined plane against another pin in a sleeve bearing. This pin transmitted the movement to the plunger (F_z). This particular mechanism was chosen for simplicity of manufacturing, as the inclined plane and boreholes for the sleeve bearings could be incorporated within the additively manufactured component that also contained the mountings for the MSM sticks. For the prototype here, a bearing ball with a diameter of 3 mm was chosen. The sleeve bearings were made from material with inner diameters of 3 mm and 2 mm for the horizontal and vertical bearings, respectively.

The incline angle of 60° resulted in a transmission ratio of tan(60°) = 1.73. With a nominal stroke of the MSM sticks of 1 mm (5% strain), the transmission created a plunger movement of 1.7 mm. The design of this variant can be seen in Figure 13, with the MSM sticks highlighted in blue. For designing the magnetic circuit, sufficient flux in the MSM sticks was the first goal. The initial simulation results showed that achieving the magnetic flux density in the MSM sticks was unproblematic due to the correlating orientation of the MSM sticks' easy axis and the magnetic field provided by the coil. A sufficiently high magnetic flux density could be achieved in the MSM sticks even with quite low electrical excitations. Since the inner diameter of the core was defined by the size of the sticks and transmission system, the resulting coil was rather large as well. From FEA simulations, a necessary magnetic excitation of around 1250 AW was necessary to achieve 850 mT in the MSM sticks, which was expected to suffice for full elongation. With a wire diameter of 0.5 mm and 1000 turns, a current of about 2.3 A was expected for the coil used. At the two ends of the MSM sticks, the flux density decreased accordingly, since the magnetic field was weakest here.

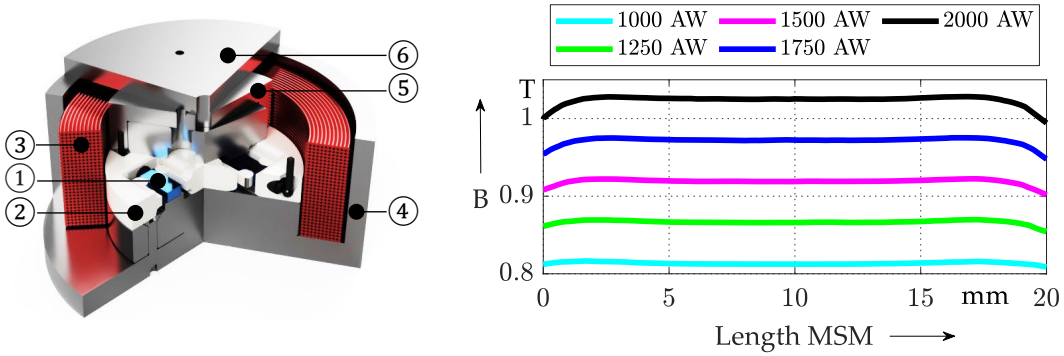

(**a**) Rendering of the horizontal setup (**b**) Simulated flux density of the horizontal setup

Figure 13. Design rendering and flux density over MSM stick length of the horizontal setup. The section of (**a**) in blue shows one of two integrated MSM sticks (①), which are embedded in the mounting (②) shown in white. Together, the assembly is placed in the center of the coil (③) and the solenoid body (④). The assembly further can actively lift the plunger (⑤) with a transmission defined by design in the axis of rotation. The armature (⑥) rests on top of the horizontal setup here.

5.3. CAE Prototyping for the Vertical Setup

The challenge for this setup was to provide the required flux density in the sticks, since the magnetic field of the coil has to be tilted by 90°. For the best possible realization of this task, a design study with six different concepts dealing with the magnetic circuit design was investigated prior to the actual designing process. This step was necessary since the initial simulation results showed that achieving magnetic flux density in the MSM sticks was problematic. Figure 14 shows the different concepts, which were compared by FEA simulation. The red bars in the concepts in Figure 14 are mechanical transmission elements that are non-ferromagnetic, and the MSM sticks are displayed in blue.

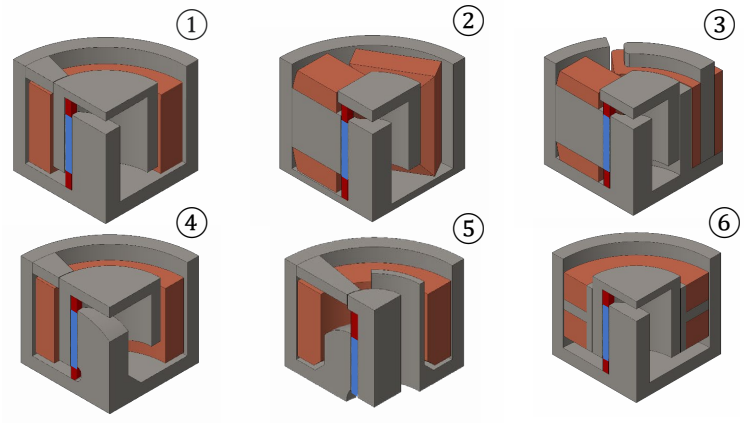

Figure 14. Concepts 1-6 of the design study for the vertical setup.

The quality criteria for the design study were, in addition to the forces on the plunger and armature and the magnetic flux density in the two MSM sticks, the lowest possible complexity of production and assembly. Each parameter was assigned a weighting. An overall design score (technical value x) was derived from the weighting and points awarded. In the following formula, w describes the weighting and p stands for awarded points, with p_{max} = 6 being the maximum score.

$$x = \frac{w_1 p_1 + w_2 p_2 + ... + w_n p_n}{(w_1 + w_2 + ... + w g_n) \cdot p_{max}} \quad (3)$$

The concepts were evaluated and weighted in different categories based on the simulation results. Table 5 shows the different parameters that were used to determine each concept's performance.

Table 5. Description of the parameters for the design study for the vertical setup.

Parameters	Description	Unit	Aim	Weighting
$F_{m,2}$	Maxwell's tensile force on the armature in step 2 (the 'steps' to describe the parameters refer to Figure 7)	N	↑	0.16
$\Delta F_{m,12}$	Difference of Maxwell's tensile force on the anchor between step 1 and step 2	N	↑	0.12
$F_{m,4}$	Maximum holding force of the solenoid in step 4	N	↑	0.14
$B_{MSM,1}$	Y-component of the magnetic flux density, the average value of which is formed over the measuring area immediately in front of the MSM stick in state 1	T	↑	0.16
$\Delta B_{MSM,1}$	Difference of the mean value of the Y-component of the magnetic flux density between the two measuring surfaces in state 1	T	↓	0.12
$B_{MSM,4}$	Magnetic flux density in step 4	T	↑	0.07
$F_{m,2,d=10}$	Maxwell's tensile force on the armature in step 2 at $\delta = 10$ mm	N	↑	0.05
$\Delta B_{d=10}$	Reduction of the magnetic flux density at the measuring surfaces of the MSM sticks at $\delta = 10$ mm	T	↓	0.05
s	Preload on the individual MSM stick at $\delta = 10$ mm	N/mm^2	↓	0.10
Effort for design, manufacturing and assembly (Designing)		-	↓	0.03

In order to create good comparability, some basic conditions applied to each concept. Uniform dimensions of the solenoid body were selected, and an active air gap of 5 mm was defined. At the end of the investigation, the air gap was then increased to 10 mm to determine whether an attraction was still possible with a doubled air gap. The air gap to hold the MSM sticks was identical in all concepts at 3.1 mm and a current of 1 A was specified for the magnetostatic simulation. Furthermore, each concept was designed symmetrically to the X and Y axis. The Z axis described the rotation axis in this case. In order to be able to weigh the individual concepts against each other, the individual parameters were given a weighting. This weighting was intended to serve as a measure of the best possible suitability of the respective concept and merely served as an indication of which concept offered the highest potential. This concept was subsequently elaborated in a detailed design. Table 6 contains the results of the FEA simulation study with data received from simulation and a rating based on the weighing and points awarded.

Table 6. Results of the design study for the vertical setup.

	Units	Concept 1	Concept 2	Concept 3	Concept 4	Concept 5	Concept 6
windings 1	-	1814	898	737	1584	1948	772
windings 2	-	-	576	742	-	-	772
$F_{m,2}$	N	−26.04	−5.70	−7.63	−18.30	−29.09	−20.56
$\Delta F_{m,12}$	Points	5	0	1	2	6	3
	N	−5.2	−1.73	−0.87	−4.41	−7.25	−5.86
$F_{m,4}$	Points	3	1	0	2	6	4
	N	−906.38	−411.13	−923.78	−802.98	−853.81	−1102.25
$B_{MSM,1}$	Points	3	0	4	1	2	5
	T	0.61	0.67	0.64	0.66	0.59	0.55
$\Delta B_{MSM,1}$	Points	3	6	4	5	2	1
	T	0.1	0 T	0.02	0.05	0.03	0.08
	Points	1	6	5	3	4	2

Table 6. *Cont.*

	Units	Concept 1	Concept 2	Concept 3	Concept 4	Concept 5	Concept 6
$B_{MSM,4}$	T	0.67	0.74	0.56	0.84	0.84	0.58
$F_{m,2,d=10}$	Points	4	5	1	6	6	2
	N	−6.14	−1.23	−1.46	−4.25	−7.51	−4.36
$\Delta B_{d=10}$	Points	5	0	1	2	6	3
	T	0.03	0	0	0.04	0.05	0.01
s	Points	4	6	6	3	3	5
	N/mm^2	0.13	0.03	0.04	0.05	0	0.19
Designing	Points	2	5	4	3	6	1
	Points	6	1	4	1	2	5
x (Acc. to Formula (3))		0.55	0.5	0.48	0.48	0.72	0.48

As result of this design study, the winning concept, concept 5 in Figure 14, was selected and designed in detail. The design and construction of the actuator have already been described in detail in [1]. In the final vertical setup, shown in Figure 15a, the direction of extension of the MSM sticks (displayed in blue) coincided with the vertical direction of movement of the plunger and armature, respectively. Due to manufacturing reasons, the cylindrical solenoid body was separated from the base plate, which did not hinder the functionality at this point.

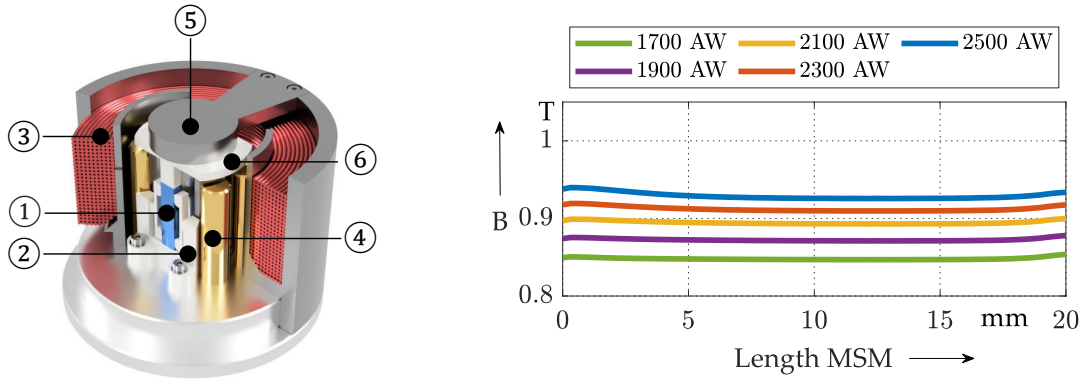

(**a**) Rendering of the vertical setup (**b**) Simulated flux density of the vertical setup

Figure 15. Design rendering and flux density over MSM stick length of the vertical setup. The section of (**a**) shows one of two integrated MSM sticks (①) in blue, which is integrated in a spring joint (②), shown in white. Together, the assembly is centered inside of the coil (③). The assembly, guided by four brass cylinders (④), can actively lift the plunger (⑤) in the axis of rotation by passing the strain of the MSM sticks to the operator (⑥) made of aluminum and thus to the ferromagnetic plunger.

In order for the MSM sticks to be able to apply their maximum elongation of 1 mm, it was important that the MSM sticks were exposed to a sufficiently strong magnetic field in the preferred orientation. The structure was provided with additional flux guiding parts to increase the magnetic flux through the sticks as well as to increase the attraction force on the armature. The elongation that occurred was passed on to an aluminum spacer, which continued to move the plunger to the forward end position. The plunger had a cylindrical flange at its end with a surface area as large as possible to maximize Maxwell's tensile force for attracting the armature. The plunger was guided in its movement by vertically arranged rods made of brass, which allowed the vertical movement under highly minimized friction. Due to its parallelogram-shaped design, the plunger touched only one theoretical line per rod. Tilting or twisting of the plunger was thus avoided and the movement could be reliably carried out. At 0.355 mm, the selected coil wire was smaller

than in the design with horizontally arranged MSM sticks where the diameter was 0.5 mm. This resulted in an increased ohmic resistance of the coil with approx. 2000 turns and therefore a larger electrical excitation required to achieve the desired flux density in the MSM material. Figure 15b shows that at least 1700 AW was required to achieve a flux density >850 mT in the MSM sticks. It is worth noting that at the ends of the MSM sticks, the magnetic field and thus the magnetic flux density did not decrease at all. As a result, homogeneous elongation throughout the MSM sticks is expected.

5.4. Presentation of the Manufactured Prototypes

After the various design processes were completed, the first real prototypes for both setups were manufactured. Figure 16 shows the horizontal setup on the left and the vertical setup on the right. Since the horizontal setup generally had a very nested structure, it is in the disassembled state in Figure 16. For the horizontal setup, the MSM sticks are located in a holder (green), which was produced using the 3D printing process. Also located in this part of the assembly are the bearing balls with the inclined plane for passing on the vertical ram movement. The green receptacle is located between the solenoid body and the inner tappet package. The spool is also inserted into the solenoid body. The vertical setup with the aluminum platform is easier to view in the assembled state. Only the inner part, shown on the right, has to be integrated into the cylindrical setup. The aluminum spacer, which transmits the strain of the MSM sticks to the ferromagnetic plunger, is easily recognizable. The flux guide parts, which were designed in the concept phase in Figure 14, could be adopted in the design.

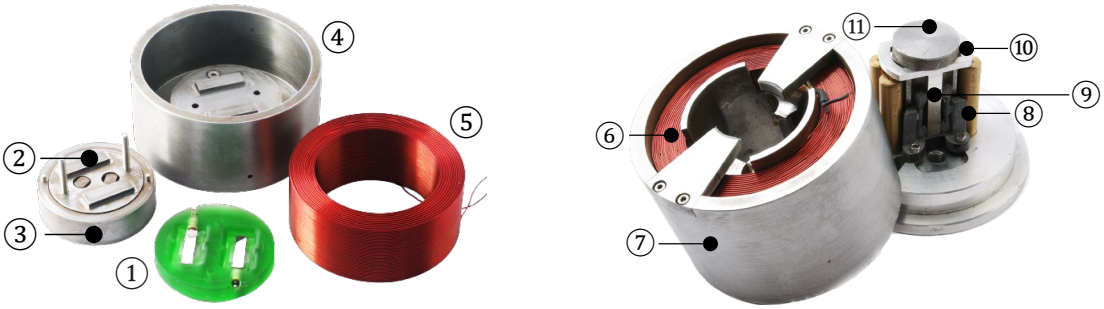

(**a**) Horizontal setup (dismantled)

(**b**) Assembled vertical setup (partially assembled)

Figure 16. Built prototypes. In (**a**), the mounting of the two MSM sticks for the horizontal setup (①) is shown in green. Both MSM sticks as well as the balls used for transmission are embedded in this mounting. The upper part of the inner flux guide (②), the plunger (③), as well as the solenoid body (④) and the coil (⑤), are shown. (**b**) shows the vertical setup of the prototype. The coil (⑥) is integrated in the solenoid body (⑦) and the brass cylinders (⑧) provide guidance for the inner assembly consisting of the MSM sticks (⑨), the operator (⑩) and the plunger (⑪).

6. Characterization

This chapter will first explain the measurement setup for the force and current measurements and then discuss the measurement results. Regarding the results presented in Section 6.2, it should be mentioned that both actuators were built with the aim of underpinning their respective functionality and demonstrating a general mode of operation. The recorded results of the two actuators can therefore only be compared qualitatively and cannot be put into relation quantitatively, since they were dimensioned differently. Differences in the magnetic field design, including the external dimensions, the dimensioning of the coil, and other factors cause deviations in the measurements. If the actuators are to be designed for a specific application with known requirements, the characteristic curves can be adapted in detail and optimized actuators can be built.

6.1. The Measurement Setups

Two different test stands were set up for collecting the measurement data. The first test stand, shown in Figure 17a, was a table-top testing machine with the vertical prototype built into it.

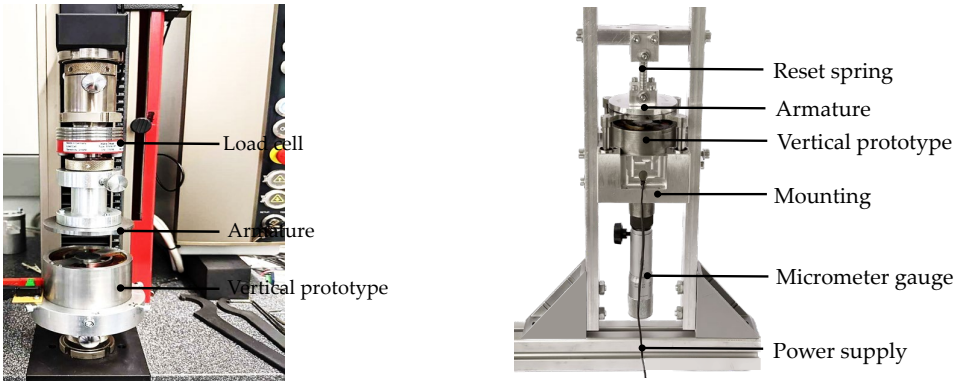

(**a**) Force–displacement measurement setup (**b**) Current–displacement measurement setup

Figure 17. The machine shown in (**a**) is equipped with a load cell and carries the armature at the lower end of the crosshead. The armature is moved quasi-statically on the respective prototypes (shown here for the vertical setup) when the coil is energized by controlled current and the applied force is measured. (**b**) shows the setup for a dynamic measurement where the armature is not dependent on the movement of a crosshead. The armature is spring-mounted and the air gap between armature and actuator can be realized by raising or lowering the actuator through the micrometer gauge. Shown is an example of the test for the vertical prototype. The current required to attract the armature with a variable air gap is measured.

The armature was connected to the crosshead of the machine (ZwickiLine table-top testing machine 1.5 kN; www.zwickroell.com (accessed on 14 August 2023) with mounted load cell (ZwickRoell Load Cell XForce HP 1000 N)). As soon as the measurement was started, the force measurement and the output of an IO-box (ZwickRoell I/O-Modul for testXpert III) were enabled simultaneously. The signal from the IO box was fed to a controllable power supply unit (power supply: Rohde&Schwarz NGP 822; www.rohde-schwarz.com (accessed on 14 August 2023)) and the solenoid was subsequently energized. The current was controlled by the power supply unit to compensate for the inevitable heating of the coil during the measurement process. As the measurement progressed, the crosshead with the armature moved downwards quasi-statically and measurement data were recorded until the armature finally rested on the solenoid body.

The measurement to determine the current–displacement relation can be seen in Figure 17b. Here, the armature was mounted on a rigid crosshead by means of a return spring and guided by four guide rods with recirculating ball bushings. The vertical setup was located in a mounting to which the micrometer gauge was also connected on the bottom. With this, it was possible to adjust the height of the solenoid and thus to obtain a specific air gap to the armature.

6.2. Presentation and Discussion of the Results

6.2.1. Force–Displacement Characteristic

The classic force–displacement characteristic of solenoids is referred to by users for classification and evaluation of an application. For a static design, the characteristic should always be situated above the counterforce, for example, of a reset spring. The first measurement results discussed here are the measured force–displacement characteristics for both setups using a table-top testing machine. Figure 18 shows the measurement results for both actuators discussed in this paper for an excitation of approx. 2500 AW, to maintain a certain comparability of the setups.

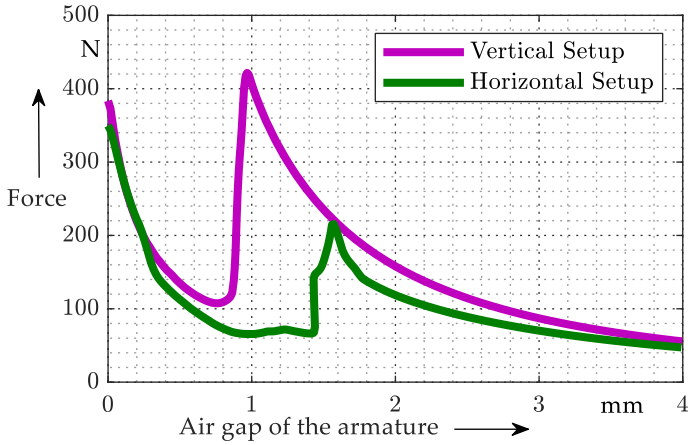

Figure 18. Measurement results for the force–displacement characteristic. The drop in force is suspected to be due to the damping effect of the MSM sticks during compression, to planar magnetic flux and thus reluctance force not acting in the axial direction, and to local magnetic saturation phenomena in the plunger of the actuator.

This corresponded to 1.2 A at 2090 turns for the vertical setup and 2.3 A at 1074 turns for the horizontal setup. The characteristic curve of the actuator with vertical MSM stick setup showed an anticipated local maximum of the force on the armature at an air gap of 1 mm. Since the MSM stick could perform an active stroke of 1 mm in this case, the local maximum was found at this point. As soon as the armature touches the plunger, step 3 in Figure 7, the magnetic flux not only propagates in the z-axis, but also proceeds in the planar plane of the x- and y-axis. The magnetic flux in this plane does not provide a force action in the z-axis direction, and therefore does not contribute to the characteristic curve and provides for the lowering of the force. In [10], this condition was also observed for different pairings of armature and armature-counterpart, which supports the plausibility of this measurement result.

Furthermore, it was observed in [1] that the compression of the MSM sticks in the presence of a magnetic field by an energized coil leads to an additional reduction in the force on the armature. Thus, a force of up to 180 N can be absorbed by the two MSM sticks for the vertical setup under the given general conditions of the measurement, but this does not fully explain the reduction in the force by approx. 300 N as observed in Figure 18. The above-described course of the magnetic flux with the corresponding observable force direction, according to [10], has a great influence. For instance, an equivalent force–displacement characteristic could be observed in [4], whereas the use of MSM sticks in the developed solenoid was completely excluded. It remains to be stated at this point that the lowering of the force is suspected to be due to several mutually influencing factors.

The characteristic curve increased as the air gap decreased and reached its maximum at approx. 380 N for the vertical structure in the closed state. This maximum was about 40 N below the absolute maximum at 1 mm of approx. 420 N. The conditions described also applied for the structure with the horizontal MSM sticks setup. Here, however, it was noticeable that the local maximum was located at an air gap of approx. 1.7 mm. Due to the transmission ratio made possible by the design with horizontal MSM sticks, the characteristic curve could be shifted into this range. By appropriate design, the characteristic curve can thus be shifted, within limits, into the preferred range, as mentioned in Figure 2. The characteristic curve increased for the horizontal setup when the air gap of the armature was reduced and reached its absolute maximum at approx. 340 N here. The shift of the characteristic curve to the right towards a larger air gap was noticeable for both setups. This behavior was expected from the result of the modeling in Matlab/Simulink. In the real measurement, it was possible to compress the stretched MSM sticks in each case and to observe a lowering of the force due to the magnetic flux deviating into the horizontal plane. The compression of the MSM sticks was not taken into account in the

Matlab/Simulink modeling, and the curve did not show a lowering of the force, since the movement was interrupted upon contact with the core of the solenoid. In principle, however, the measurement confirmed the hypothesis from the modeling very well.

6.2.2. Current–Displacement Characteristic

For the current–air gap characteristic, a hypothesis was also derived from the results of the Matlab/Simulink model in Figure 6. Thus, with a suitable design of the magnetic circuit, the characteristic curve should be shifted to the right due to the active stroke that has occurred because of the elongation of the MSM sticks. Attraction of the armature can occur at a smaller current due to the reduced air gap. For the measurement, a digital oscilloscope (oscilloscope: Rohde&Schwarz RTM3K-24M; www.rohde-schwarz.com)) and current clamp (current clamp: Fluke i30s; www.fluke.com (accessed on 14 August 2023)) were used to observe the switching process while gradually changing the air gap of the armature. A precision micrometer (precision micrometer: Hartig 3585 S2 0-60; www.hartig-germany.com (accessed on 14 August 2023)) was used to change the air gap from 4 mm to the closed state, and the current required for a switching operation was noted for five measurements per state. This procedure was carried out for the real actuator and a comparison setup. In the comparison setup, the vertical and horizontal setups were changed so that the active stroke was no longer passed on to the plunger by the MSM stick elongation. In the vertical setup, the aluminum spacer was removed, and in the horizontal setup, the force redirection balls were removed. However, the magnetic circuit remained identical to the original setup in both comparative setups.

The left side of Figure 19 shows the measurement results for the horizontal setup.

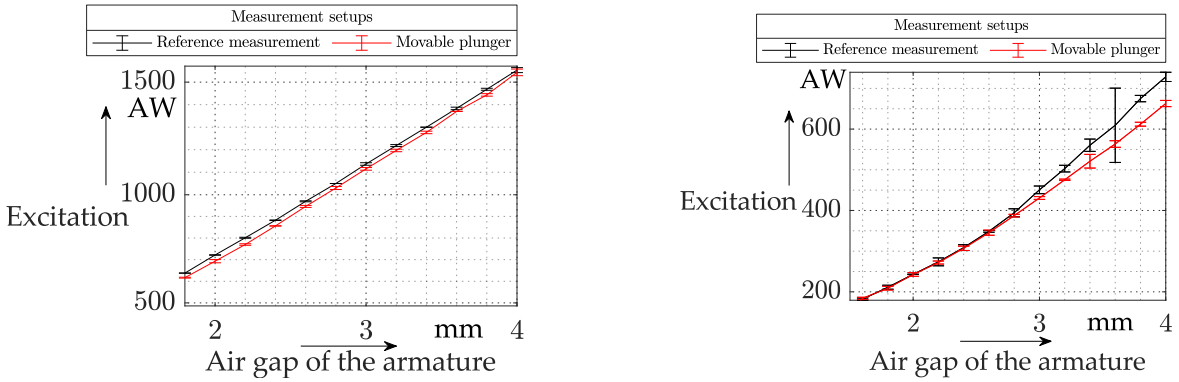

Figure 19. Measurement results for the current–displacement characteristic.

The red characteristic curve represents the result for the original setup and the reference measurement is shown in black. The red characteristic curve runs parallel and below the black characteristic curve and does not show the behavior that was expected from the results of the Matlab/Simulink model. The situation is different on the right side of Figure 18, which shows the behavior of the actuator with vertical setup of the MSM sticks. Here, it is noticeable that the red characteristic curve with moving plunger shows the behavior expected from the model for an air gap of about 2.8 mm ongoing. The characteristic curve bends downward and thus significantly reduces the current required to attract the armature plate up to 9% at an air gap of 4 mm. The reason for the unexpected behavior of the actuator with horizontal setup was magnetic saturation. A closer look at the FEA simulation revealed areas in the plunger that exhibited strong saturation. A redesign of the magnetic circuit should be considered to improve the functionality of this setup. In the vertical setup, no unexpected saturations occurred in the magnetic circuit and the operation met the expectations derived from the Matlab/Simulink model.

7. Discussion and Conclusions

The two actuators presented in this contribution showed that actuators with an adjustable core can influence the characteristic curves of an electromagnet in a useful way. Both the force–displacement characteristic and the current–displacement characteristic could be modified. The active stroke of the plunger was realized here with MSM material, but IKFF is researching actuators that do not require such material [4]. This would be, among other things, a saving of costs and an extension of the field of application for the actuators, since MSM alloys are expensive and temperature-sensitive. The lower power consumption shown for switching operations means that actuators with an active core can be miniaturized, for example, by using MSM sticks. In particular, the coil used to drive the solenoid can be made smaller, thus reducing costs in terms of material requirements.

For the actuator with horizontally arranged sticks, it is necessary to go through the magnetic design process again, and the measurement results have not been sufficient up to now. Here, it could be beneficial to go through a new concept phase for the design of the magnetic circuit, similar to the vertical setup. Based on this, a new prototype could subsequently be designed that shows better functionality in the dynamic measurements than the previous one.

In contrast, the actuator with vertical setup confirmed what the Matlab/Simulink model indicated at the beginning of the study. Both actuators are to be understood as proofs of concept and are not claimed to be ready for commercialization. It is also up to the user whether a translation of the limited stroke is required. Generally, based on the simulation results, the actuator with horizontal setup offers more possibilities for miniaturization, including translation. This will be investigated in future research.

Author Contributions: Conceptualization, M.M. and M.H.; methodology, M.M. and M.H.; validation, M.M. and M.H.; formal analysis, M.M.; investigation, M.M. and M.H.; resources, M.M. and M.H.; data curation, M.M. and M.H.; writing—original draft preparation, M.M. and M.H.; writing—review and editing, B.G.; visualization, M.M.; supervision, B.G.; project administration, M.M.; funding acquisition, B.G. All authors have read and agreed to the published version of the manuscript.

Funding: This research received no external funding.

Institutional Review Board Statement: Not applicable.

Data Availability Statement: Data presented in this study are available on request from the corresponding author.

Conflicts of Interest: The authors declare no conflict of interest.

References

1. Mauch, M.; Hutter, M.; Gundelsweiler, B. *Development of an Electromagnetic Actuator with Magnetic Shape Memory Active Core for Stroke Enlargement and Noise Reduction*; VDE Verlag: Berlin, Germany, 2021.
2. Gundelsweiler, B.; Mauch, M.; Raab, M. Aktor Mit Aktivem Kern. Germany Patent DE102019218567B3_1, 6 May 2021.
3. Gundelsweiler, B.; Mauch, M. Elektromagnetischer Hub- und/oder Haft-Aktor. Germany Patent DE102021124654A1, 3 November 2022.
4. Mauch, M.; Gundelsweiler, B. Design of a hybrid electromagnetic switching/holding solenoid with adjustable core. In Proceedings of the IKMT 2022, 13. GMM/ETG-Symposium. Linz, Austria, 14–15 September 2022; pp. 1–6.
5. Ullakko, K.; Huang, J.K.; Kantner, C.; O'handley, R.C.; Kokorin, V.V. Large magnetic-field-induced strains in Ni_2MnGa single crystals. *Appl. Phys. Lett.* **1996**, *69*, 1966–1968. [CrossRef]
6. ETO GRUPPE TECHNOLOGIES GmbH. Magnetoshape. Available online: https://www.etogruppe.com/unternehmen/magnetoshape-r.html (accessed on 27 March 2023).
7. Hubert, A.; Calchand, N.; Le Gorrec, Y.; Gauthier, J.-Y. Magnetic Shape Memory Alloys as smart materials for micro-positioning devices. *Adv. Electromagn.* **2012**, *1*, 75–84. [CrossRef]
8. Schlüter, K.; Holz, B.; Raatz, A. Principle Design of Actuators Driven by Magnetic Shape Memory Alloys. *Adv. Eng. Mater.* **2012**, *14*, 682–686. [CrossRef]
9. Linsmeier, K.-D. *Elektromagnetische Aktoren: Physikalische Grundlagen, Bauarten, Anwendungen*; Die Bibliothek der Technik 118; Verlag Moderne Industrie: Landsberg am Lech, Germany, 1995.

10. Kallenbach, E.; Eick, R.; Ströhla, T.; Feindt, K.; Kallenbach, M.; Radler, O. *Elektromagnete*; Springer Fachmedien Wiesbaden: Wiesbaden, Germany, 2018.
11. Gabdullin, N.; Khan, S.H. Review of properties of magnetic shape memory (MSM) alloys and MSM actuator designs. *J. Phys. Conf. Ser.* **2015**, *588*, 012052. [CrossRef]
12. Happel, J.; Pagounis, E.; Schnetzler, R.; Heider, J.; Laufenberg, M. Multistable proportional valve: An energy efficient approach for high temperature passive magnetic shape memory applications. In Proceedings of the ACTUATOR; International Conference and Exhibition on New Actuator Systems and Applications 2021, Online, 17–19 February 2021; pp. 1–3.
13. Raab, M.; Hutter, M.; Kazi, A.; Schinkoethe, W.; Gundelsweiler, B. Magnetically Levitated Linear Drive Using an Active Gravity Compensation Based on Hybrid Shape Memory Actuators. *IEEE/ASME Trans. Mechatron.* **2021**, *26*, 1380–1391. [CrossRef]
14. Holz, B.; Riccardi, L.; Janocha, H.; Naso, D. MSM Actuator: Design Rules and Control Strategies. *Adv. Eng. Mater.* **2012**, *14*, 668–681. [CrossRef]
15. Gauthier, J.-Y.; Hubert, A.; Abadie, J.; Chailet, N.; Lexcellent, C. Magnetic Shape Memory Alloy and Actuator Design. In Proceedings of the 5th International Workshop on Microfactories, IWMF'06, Besançon, France, 25–27 October 2006.
16. Schiepp, T.; Pagounis, E.; Laufenberg, M. Magnetic Shape Memory Actuators for Fluidic Applications. In Proceedings of the 9th International Fluid Power Conference, Aachen, Germany, 24–26 March 2014. [CrossRef]
17. Effner, A.; Zawada, T.; Weber, J. A Design Approach for a Valve Based on a Magnetic Shape Memory Actuator. *Shape Mem. Superelasticity* **2020**, *6*, 107–114. [CrossRef]
18. Wegener, K.; Blumenthal, P.; Raatz, A. Development of a miniaturized clamping device driven by magnetic shape memory alloys. *J. Intell. Mater. Syst. Struct.* **2014**, *25*, 1062–1068. [CrossRef]
19. Gauthier, J.Y.; Hubert, A.; Abadie, J.; Lexcellent, C.; Chaillet, N. Multistable actuator based on magnetic shape memory alloy. In Proceedings of the 10th International Conference on New Actuators, ACTUATOR'06, Bremen, Germany, 14–16 June 2006; pp. 787–790.
20. Smith, A.R.; Fologea, D.; Mullner, P. Magnetically Driven Pump for Solid-state Microfluidic Flow Control. In Proceedings of the ACTUATOR 2018; 16th International Conference on New Actuators, Bremen, Germany, 25–27 June 2018; pp. 1–2.
21. Happel, J.; Schnetzler, R.; Laufenberg, M. Intelligent force-controlled miniature gripper driven by magnetic shape memory alloy. In Proceedings of the ACTUATOR 2022; International Conference and Exhibition on New Actuator Systems and Applications, Mannheim, Germany, 29–30 June 2022.
22. Hutter, M.; Gundelsweiler, B. Analysis of the impact of mechanical guidance on active MSM-stick elongation behavior. In Proceedings of the ACTUATOR 2022; International Conference and Exhibition on New Actuator Systems and Applications, Mannheim, Germany, 29–30 June 2022; pp. 1–4.